

Article

Promising Eco-Friendly Nanoparticles for Managing Bottom Rot Disease in Lettuce (*Lactuca sativa* var. *longifolia*)

Nashwa A. H. Fetyan ¹, Tarek A. Essa ² , Tamer M. Salem ³, Ahmed Aboueloyoun Taha ³, Samah Fawzy Elgobashy ², Nagwa A. Tharwat ⁴ and Tamer Elsakhawy ^{1,*} 

¹ Agricultural Microbiology Research Department, Soils, Water and Environment Research Institute, Agriculture Research Center, Giza 12619, Egypt; nashwa.fetyan@arc.sci.eg

² Plant Pathology Research Institute, Agricultural Research Center, Giza 12619, Egypt; tarekessa69@gmail.com (T.A.E.); samahelgobashy@gmail.com (S.F.E.)

³ Environment Research Department, Soils, Water and Environment Research Institute, Agriculture Research Center, Giza 12619, Egypt; tamer_salem43@yahoo.com (T.M.S.); ahmadoyoun@gmail.com (A.A.T.)

⁴ Botany and Microbiology Department, Faculty of Science, Cairo University, Giza 12613, Egypt; nagwatharwat@yahoo.com

* Correspondence: drelsakhawy@gmail.com

Abstract: Developing innovative, eco-friendly fungicide alternatives is crucial to mitigate the substantial threat fungal pathogens pose to crop yields. In this study, we assessed the in vitro effectiveness of SiO₂, CuO, and γFe₂O₃ nanoparticles against *Rhizoctonia solani*. Furthermore, greenhouse experiments were conducted in artificially infested soil to evaluate the in vivo impact of nanoparticles under study. Two application methods were employed: soil drenching with 10 mL per pot at concentrations of 50, 100, and 200 mg L⁻¹, and seedling dipping in nanoparticle suspensions at each concentration combined with soil drench. The combined treatment of 200 mg L⁻¹ γFe₂O₃ or CuO nanoparticles showed the highest in vitro antifungal activity. Conversely, SiO₂ nanoparticles demonstrated the lowest in vitro activity. Notably, the application of 200 mg/L SiO₂ via the dipping and soil drenching methods decreased counts of silicate-solubilizing bacteria and *Azospirillum* spp. Whereas, application of 100 mg L⁻¹ γFe₂O₃ nanoparticles via soil drenching increased soil bacterial counts, and CuO nanoparticles at 50 mg L⁻¹ through dipping and soil drenching had the highest dehydrogenase value. γFe₂O₃ nanoparticles improved plant photosynthetic pigments, reduced malondialdehyde levels, and minimized membrane leakage in lettuce plants. A root anatomical study showed that 200 mg L⁻¹ CuO nanoparticles induced toxicity, whereas 200 mg L⁻¹ γFe₂O₃ or SiO₂ nanoparticles positively affected root diameter, tissue structure, and various anatomical measurements in lettuce roots. γFe₂O₃ nanoparticles hold promise as a sustainable alternative for managing crop diseases.

Keywords: metal oxides NPs; fungicide; *Rhizoctonia solani*; disease suppression



Citation: Fetyan, N.A.H.; Essa, T.A.; Salem, T.M.; Taha, A.A.; Elgobashy, S.F.; Tharwat, N.A.; Elsakhawy, T. Promising Eco-Friendly Nanoparticles for Managing Bottom Rot Disease in Lettuce (*Lactuca sativa* var. *longifolia*). *Microbiol. Res.* **2024**, *15*, 196–212. <https://doi.org/10.3390/microbiolres15010014>

Academic Editor: Ligang Zhou

Received: 26 October 2023

Revised: 9 January 2024

Accepted: 12 January 2024

Published: 16 January 2024



Copyright: © 2024 by the authors. Licensee MDPI, Basel, Switzerland. This article is an open access article distributed under the terms and conditions of the Creative Commons Attribution (CC BY) license (<https://creativecommons.org/licenses/by/4.0/>).

1. Introduction

Agriculture is the primary pillar of the developing economy, providing food for a better quality of life. The agricultural sector is currently facing a wide range of challenges, including unpredictable climate change, soil contamination with harmful environmental pollutants, such as fertilizers and pesticides, combined with the dramatic rise in food demand due to the growing global population [1]. Recent years have witnessed significant advances and innovations in agriculture to address the challenges of sustainable food security [2]. Nanomaterials have emerged as valuable tools in enhancing agricultural capabilities [3]. Globally, nanomaterial production reached 260,000–309,000 metric tons in 2010 and continued to grow, with consumption ranging from 225,060 to 585,000 metric tons between 2014 and 2019 [4]. These materials, known for their unique properties, have found increasing application in agriculture, including various types such as metal oxides, silicates, ceramics, and more [5]. Utilizing nanomaterials in agriculture aims to

reduce the use of plant protection products, minimize nutrient losses during fertilization, and optimize revenue through improved nutrient management [6]. Notably, one of the promising applications in plant pathology involves using nanomaterials to control plant diseases and enhance plant growth [7].

The soil-borne phytopathogenic fungus *Rhizoctonia solani* Kuhn (teleomorph: *Thanatephorus cucumeris* (A.B. Frank) Donk; basidiomycetes) is responsible for high yield losses in a number of economically important crops worldwide [8]. It can cause pre- and post-emergence damping off and bottom rots, commonly producing sclerotia on dead tissues [9]. *R. solani* causes bottom rot on lettuce, an economically important disease resulting in yield losses up to 70% [10]. The control of the pathogen is difficult because of its wide host range and its ability to survive as sclerotia under adverse environmental conditions. In practice, the control of diseases caused by *R. solani* relies mainly on fungicides [11]. However, increasing concern about the health and environmental hazards associated with the use of agrochemicals has resulted in the search for viable alternatives. Hence, it became very important and urgent to find effective strategies to control this disease [12].

Nanomaterials, including nano-metal, nano-metal oxides, and metal salts, possess unique properties that make them potential elicitors for enhancing antimicrobial activity against plant pathogens. Due to their large surface-to-volume ratio and small size compared to the same substances in their normal size, these nanomaterials could be effective in improving plant health and fighting against plant diseases [13–17]. Lettuce plants, susceptible to a range of soil-borne pathogenic fungi, face significant threats that can result in considerable yield and quality losses. Among these diseases, bottom rot stands out as one of the most destructive, particularly affecting lettuce plants during their head stage, causing decay, and often rendering the heads unsuitable for the market due to severe rotting. Even minor infections necessitate additional lower leaf trimming, leading to increased harvesting labor and reduced lettuce quality and head weight [18].

Copper nanoparticles (Cu NPs) are envisioned as pivotal in the next generation of nanomaterials due to their cost-effectiveness [19]. Copper oxide variants (CuO and Cu₂O) are widely used antimicrobial agents, with CuO being cost-effective, easily combinable with polymers, and possessing stable chemical and physical properties [20]. High-ionic-scale metal oxides like CuO are of particular interest for their large surface areas and crystal shapes that enhance their antimicrobial potency [21]. Additionally, copper serves as a vital plant micronutrient, contributing to plant growth and disease resistance. Copper nanoparticles (CuO NPs) influence plant nutrition and disease defense, with Cu₂ONPs acting as an effective nano-fertilizer to enhance disease resistance, as seen in systems like asparagus/fusarium crown and root rot [22].

Iron oxide nanoparticles demonstrated a substantial reduction in *Fusarium oxysporum* conidial germination rate and fungal growth, leading to a decrease in pathogen numbers on infected plants. Their pesticide effect proves effective against various pathogens, including fungi, bacteria, and viruses. Additionally, iron-oxide nanoparticles reduced fusaric acid production and increased mannitol content, thereby decreasing phytotoxin production in infected plants and resulting in a reduced disease index [23].

Besides its nutritional importance, Si stimulates plant resistance mechanisms against both biotic and abiotic stress [24]. It is known to suppress various plant diseases across crops, including multiple diseases in rice, as well as powdery mildew in wheat and cucumber [25]. Reducing Si particle size to the nano level through a safe synthesis method could enhance its efficacy in improving plant growth, resistance and suppressing plant pathogenic fungi [26].

The aim of this study was to (i): evaluate the efficacy of SiO₂, CuO, and γFe₂O₃ nanoparticles as novel fungicides against *Rhizoctonia solani*, the pathogen responsible for bottom rot disease in lettuce; (ii): to assess the impact of these nanoparticles on soil health parameters and plant responses to the treatments. The study innovatively explores the use of nanoparticles as a potent and sustainable alternative for managing crop diseases, specifically *Rhizoctonia solani*, responsible for bottom rot in lettuce. It demonstrates their ef-

fectiveness through in vitro antifungal activity, enhanced plant health, and root anatomical improvements, offering a promising, environmentally friendly fungicide alternative.

2. Materials and Methods

2.1. Synthesis of Nanomaterials

A comprehensive explanation of the synthesis methods, along with their corresponding characterization, is available in the supporting information.

2.2. Enmiration, Isolation, Identification of Fungal Pathogens Responsible for Bottom Rot

Lettuce plant samples affected by bottom rot disease were collected from El-Mansoria and Nahia fields in Giza governorate. The lower stems and roots were rinsed, sterilized with 3% sodium hypochlorite for three minutes, and placed on potato dextrose agar (PDA) medium for fungal growth. The isolated fungi were identified based on morphological characteristics, following references [27,28]. The percentage of colony frequency was calculated using Equation (1):

$$\text{The frequency(\%)} = \frac{n}{N} \times 100 \quad (1)$$

where “ n ” represents the number of colonies for each pathogen, and “ N ” is the total number of colonies. For in vivo experiments, a rice hull medium was prepared by sterilizing a mixture of rice grains, sand, and water, which was then inoculated with the fungus mycelium and incubated at 28 °C for 7 days.

2.3. Pathogenicity Tests

The fungal isolates obtained from lettuce plant samples affected by bottom rot disease (*Rhizoctonia solani* F. *oxysporum* and *F. solani*) isolates were tested for pathogenicity on lettuce (*Lactuca sativa* Var. *longifolia*) in 25 cm diameter plastic pots filled with a sterile 1:2 sand and peat moss substrate mix. Soil inoculation with *R. solani* using hull rice culture (3% *w/w*) was carried out a week before transplantation. Each treatment involved three pots, and re-isolation from the bottom was performed to fulfill Koch’s postulates. Disease incidence and severity were calculated as per [29] using Equation (2).

$$\text{Disease incidence(\%)} = \frac{\text{Number of infected plants}}{\text{Total number of plants}} \times 100 \quad (2)$$

Disease severity was evaluated based on the progression of yellowing, root rot, and overall plant decay at the end of the experiment, and recorded as the percentage of symptomatic plants. Disease severity assessment was determined using a modified 0–5 scale by [30] where 0 = 0%, 1 = 0–10%, 2 = 10–25%, 3 = 25–50%, 4 = 50–75%, and 5 = 75–100%. The disease severity percentage (DS%) was calculated based on the following Equation (3):

$$\text{Disease severity (\%)} = \frac{\sum n \times r}{5N} \times 100 \quad (3)$$

where n is the number of plants in each numerical rate, N is the total number of plants multiplied by the maximum numerical rate, and r is equal to 5.

2.4. In Vitro Examination of Antifungal Activity of the Prepared Nanomaterials

According to the pathogenicity test, *R. solani* was the most causative agent for bottom rot among other pathogens, so it was selected to complete the study. The antifungal activity of SiO₂NPs, CuONPs, Fe₂O₃ NPs, and Rizolex[®] fungicide against *R. solani* was evaluated using a modified method outlined by [31]. SiO₂NPs, CuONPs, and Fe₂O₃ NPs were added to autoclaved PDA media at concentrations of 50, 100, and 200 µg L⁻¹, while Rizolex[®] fungicide was added at a concentration of 2.5 g L⁻¹. PDA plates without any additives were set as control. Subsequently, 0.5 cm diameter disks of a 7-day-old fungal growth were

placed on the center of each Petri dish. The radial growth was measured after 7 days of incubation or when the fungal growth was completely covered in the control treatment.

The inhibition percentage was estimated using the following equation:

$$\text{degree of inhibition in radial growth (\%)} = (C - T)/C \times 100 \quad (4)$$

where C represents the mycelium growth in the control (cm), and T represents the mycelium growth in the treatments (cm).

2.5. In Vivo Examination of Antifungal Activity of the Prepared Nanomaterials

Sandy clay-loam soil was sterilized with 5% formalin and air dried for 7 days [32]. Each 25 cm diameter pot contained 4 kg of sterilized soil infected with *R. solani*. Lettuce seedlings were treated with SiO₂NPs, CuONPs, and Fe₂O₃ NPs, suspensions (50, 100, and 200 mg L⁻¹) for 2 h prior to planting. Soil drench treatments with the same solutions were administered by injecting 10 mL around the lettuce roots. Control groups received distilled water. The plants were grown to maturity using standard practices, and the incidence and severity of bottom rot disease were recorded 45 days after transplanting. Soil properties were assessed following the method by [33]. Treatments details are presented in Table 1.

Table 1. Description of the greenhouse experiment.

Treatments	Description	Treatments	Description
T1	50 mg L ⁻¹ SiO ₂ soil drench	T12	200 mg L ⁻¹ SiO ₂ roots dipping + soil drench
T2	100 mg L ⁻¹ SiO ₂ soil drench	T13	50 mg L ⁻¹ CuO roots dipping + soil drench
T3	200 mg L ⁻¹ SiO ₂ soil drench	T14	100 mg L ⁻¹ CuO roots dipping + soil drench
T4	50 mg L ⁻¹ CuO soil drench	T15	200 mg L ⁻¹ CuO roots dipping + soil drench
T5	100 mg L ⁻¹ CuO soil drench	T16	50 mg L ⁻¹ Fe ₂ O ₃ roots dipping + soil drench
T6	200 mg L ⁻¹ CuO soil drench	T17	100 mg L ⁻¹ Fe ₂ O ₃ roots dipping + soil drench
T7	50 mg L ⁻¹ Fe ₂ O ₃ soil drench	T18	200 mg L ⁻¹ Fe ₂ O ₃ roots dipping + soil drench
T8	100 mg L ⁻¹ Fe ₂ O ₃ soil drench	T19	Control (plants inoculated with fungal pathogen)
T9	200 mg L ⁻¹ Fe ₂ O ₃ soil drench	T20	Control (plants inoculated with fungal pathogen) + Rizolex® 2.5 g L ⁻¹
T10	50 mg L ⁻¹ SiO ₂ roots dipping + soil drench	T21	Control (healthy plants)
T11	100 mg L ⁻¹ SiO ₂ roots dipping + soil drench		

All soil drench treatments received 10 mL of a specific solution of above concentrations.

2.6. Soil Biological Activities

To evaluate the ecological impact of nanomaterials under study, the following biological measurements were conducted.

2.6.1. Microbial Populations

To assess the total microbial count, rhizosphere soil samples were collected 45 days after transplanting and stored at 4 °C to maintain microbiological activity. The plate count technique was employed using potato dextrose agar medium (PDA) [34] and nutrient agar medium [35] for enumerating total fungi and bacteria, respectively. Serial dilution and standard count techniques were utilized to isolate and enumerate free-living nitrogen fixers, phosphate-solubilizing bacteria, and silicate-solubilizing bacteria. Free-living nitrogen fixers were cultured on N-free media, *Azospirillum* spp. on N-deficient medium [36], *Azotobacter* spp. on Modified Ashby's broth medium [37], phosphate solubilizers on Pikovskaya's agar medium [38], and silicate bacteria on Aleksandrov's agar medium [39].

2.6.2. Soil Enzymes Activities

The dehydrogenase activity in the soil was determined using the method described by [40]. The urease activity was measured following the protocol by [41]. The alkaline phosphatase in the soil was assessed according to [42]. The nitrogenase activity in the plant rhizosphere was determined by the acetylene reduction method according to [36].

2.7. Plant Sampling and Analysis

2.7.1. Estimation of Photosynthetic Pigments

To determine the total chlorophyll, chlorophyll a, chlorophyll b, and carotenoid contents, 0.5 g of leaf tissue was extracted using 10 mL of 80% acetone. The pigment estimation was carried out using a spectrophotometer (UV1901PC) at 645, 663, and 470 nm following the method of [43]. Acetone (80%) was used as the blank. The equations for the calculations are as follows:

$$\text{Total chlorophyll (mg/mL)} = 0.0202 \times A_{645} + 0.00802 \times A_{663}$$

$$\text{Chlorophyll a (mg/mL)} = 0.0127 \times A_{663} - 0.0027 \times A_{645}$$

$$\text{Chlorophyll b (mg/mL)} = 0.0229 \times A_{645} - 0.0046 \times A_{663}$$

$$\text{Carotenoid (mg/mL)} = A_{470} \times 0.1140 \times A_{663} - 0.6380 \times A_{645}$$

2.7.2. Cell Membrane Stability Index

Membrane stability was assessed by measuring lipid peroxidation products, indicated by thiobarbituric acid (TBA) reactive substances equivalent to malondialdehyde (MDA), following [44]. Electrolyte leakage (EL) from leaf tissue was measured using a conductivity meter (Adwa-AD32). Three replicates were used, where samples were immersed in de-ionized water, and the conductivity was measured immediately and after 1 h. The electrolyte leakage rate was calculated as the net conductivity after 1 h divided by the total conductivity after boiling, as described by [45].

2.7.3. Anatomical Structure

Anatomical preparations of root cross-sections were conducted using the paraffin embedding method according to [46]. The root midribs of infected and healthy lettuce plants were killed and fixed for at least 48 h in formalin glacial acetic acid before being dehydrated. They were then serially sectioned by a rotary microtome at 20 μm thickness, and finally double stained with crystal violet and erythrosine, cleared in carbol xylene, and mounted in Canada balsam. Observations of the anatomy slides were performed using a light microscope (CX22LED, Olympus) and documented using a digital microscope camera (Optilab Advance V2, Miconos).

2.8. Statistical Analysis

The collected data were analyzed using analysis of variance (ANOVA) based on a randomized complete block design (RCBD). Statistical analysis was performed using WASP software Version 12.4.12.79. To compare the mean differences between treatments, the Least Significant Difference (LSD) test was employed. The significance level was set at $p < 0.05$ [47].

3. Results and Discussion

3.1. Characterization of Synthesized Nanomaterials

Nano silica was prepared according to the method described by [48], Magnetic nanoparticles (MNPs) was prepared according to [49]. Nano-Cu was prepared by chemical precipitation according to the procedure described by [50,51]. Comprehensive Scanning Electron Microscope (SEM) for each type of the prepared nanomaterials can be found in the Supplementary Materials.

3.2. Isolation and Frequency Percentages of Causal Agents of Lettuce Bottom Rot

Table 2 presents data on the isolation and frequency percentages of causal agents of lettuce bottom rot. The results indicate that two fungal genera were identified from the discolored bottom rot of lettuce cv. Nader collected from four villages (El Mansoria and Nahia) in Giza governorate. The fungi were identified based on morphological criteria and

microscopic features, and were identified as *Fusarium oxysporum* Schlecht, *F. solani*, and *Rhizoctonia solani* Kuhn. *Rhizoctonia solani* was the most prominent fungi, accounting for 63.64% of the total isolates. *Fusarium solani* was also frequently isolated, with a frequency of 21.21%, followed by *F. oxysporum*, which was isolated at a lower frequency of 15.15%.

Table 2. Isolation and frequency percentages of causal agents of lettuce bottom rot.

Isolates	El Mansoryh		Nahia		Total	
	No.	Frequency %	No.	Frequency %	No.	Frequency %
<i>Rhizoctonia solani</i>	12	70.53%	9	60.00	21	63.64%
<i>Fusarium solani</i>	3	17.91%	4	26.67	7	21.21%
<i>Fusarium oxysporum</i>	2	11.56%	2	13.33	5	15.15%
Total	17	100%	15	100	33	100%
LSD at 0.05%		20.06		12.89		

3.3. Pathogenicity Test

The data presented in Table 3 indicate that the Nader cultivar is susceptible to *Rhizoctonia solani*, as evidenced by the similar symptoms observed in the field, including discoloration of the internal tissues at the bottom. *R. solani* was successfully isolated from the symptomatic tissues and recorded a high disease index and severity on Nader cultivar, at 83.33% and 64.77%, respectively. On the other hand, *Fusarium solani* showed a low disease index and severity, at 33.33% and 3.24%, respectively. The lowest disease incidence was observed when Nader cultivar was inoculated with *F. oxysporum*.

Table 3. Pathogenicity test of causal agents of lettuce bottom rot.

Isolates	Disease Incidence %	Disease Severity %
<i>Rhizoctonia solani</i>	83.33	64.77
<i>Fusarium solani</i>	33.33	3.24
<i>Fusarium oxysporum</i>	16.67	1.48
Control	0.00	0.00
LSD at 0.05%	21.25	2.74

3.4. Antifungal Performance of Nano-SiO₂, Nano-γFe₂O₃ and Nano-Copper against *R. solani* In Vitro Experiment

Based on the in vitro experiment (Table 4), ferric and copper oxide nanoparticles exhibited moderate inhibitory effects on the mycelial growth of *R. solani* at all concentrations compared to commercial fungicide. The highest reduction in mycelium growth (23.33%) was observed with Fe₂O₃ at 200 mg L⁻¹, followed by Nano-γFe₂O₃ at 100 mg L⁻¹ (18.22% reduction) and 50 mg L⁻¹ (17.11% reduction). Nano-copper oxide at 200 mg L⁻¹ resulted in an 11.89% reduction Figure 1. However, SiO₂ nanoparticles did not affect the mycelial growth. The detrimental effects of CuO and γ-Fe₂O₃ nanoparticles on *R. solani* mycelium may be attributed to interactions with P- and S-containing molecules inside or outside fungal cells, disrupting cell wall functions, protein synthesis, and ion exchanges, ultimately leading to cell death. Previous studies have highlighted similar mechanisms of action for CuO nanoparticles [52] and iron oxide nanoparticles [53]. On the other hand, the small size and larger surface area to volume ratio of nanoparticles in addition to their ability to reduce the oxygen supply for respiration enhance their antifungal potential. Thus, CuO and γ-Fe₂O₃ nanoparticles demonstrate potential as alternative control measures against fungal pathogens affecting stored vegetables.

Table 4. Effect of the prepared nanomaterials on linear growth of *Rhizoctonia solani* on lettuce plants.

Treatments	Concentration ppm	Linear Growth	Reduction %
SiO ₂	50	9 ^a	0.0
	100	9 ^a	0.0
	200	9 ^a	0.0
CuO	50	8.26 ^{ab}	8.22
	100	8.26 ^{ab}	8.22
	200	7.93 ^{bc}	11.89
Fe ₂ O ₃	50	7.46 ^{bc}	17.11
	100	7.36 ^c	18.22
	200	6.9 ^c	23.33
Rizolex	2.5 g/L	4.5 ^d	50
Control	0	9.0 ^a	0

Different letters in the same row mean significant difference. The significance level was set at $p < 0.05$.

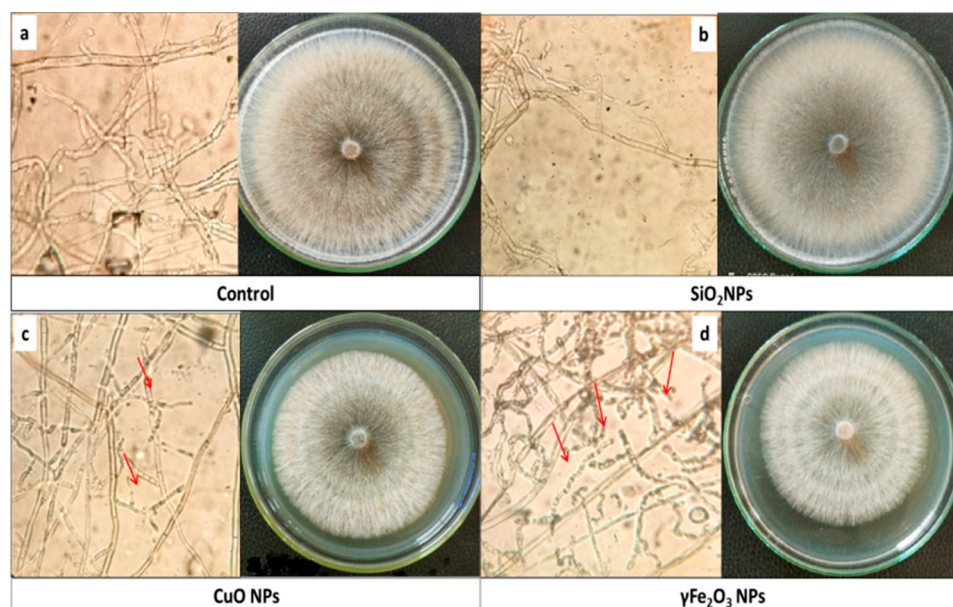


Figure 1. (a) is the control *R. solani* mycelium with right-angled branching and constriction, (b) is effect of SiO₂NPs, (c) is the effect of CuONPs, (d) is the effect of γ Fe₂O₃NPs (magnification 40 \times and red arrows pointed degradation ends).

3.5. Greenhouse Experiment

Under greenhouse conditions, SiO₂, CuO, and γ Fe₂O₃ nanoparticles were evaluated for their efficacy in controlling lettuce bottom rot disease. Physical and chemical characteristics of the used soil, revealing sandy clay–loam texture with pH 7.7, EC 2.16 ds/m, organic matter 1.58%, total nitrogen 0.13%, total phosphorus 0.025%, available phosphorus 0.005%, and total potassium 0.178%.

The results presented in Table 5 demonstrated that all tested γ Fe₂O₃ and CuO nanoparticles effectively reduced the severity of lettuce bottom rot compared to control and fungicide treatments. Significantly, γ Fe₂O₃ and CuO nanoparticles at a concentration of 200 mg L⁻¹ exhibited higher effectiveness in reducing disease severity than SiO₂ nanoparticles at a concentration of 100 mg L⁻¹ and fungicide treatments. The reduction in disease severity was 24.84% and 34.11% for γ Fe₂O₃ and CuO nanoparticles, respectively, while SiO₂ nanoparticles and fungicide treatments resulted in reductions of 36.18% and 18.32%, respectively. These findings highlight the considerable potential of γ Fe₂O₃ and CuO nanoparticles in controlling lettuce bottom rot disease.

Table 5. Effect of the nanomaterials on head rot of lettuce plants under greenhouse conditions.

Treatments	Disease Incidence %	Disease Severity %	Fresh Weight (g)	Dry Weight (g)
T1	50.0 ^{cd}	36.50 ^e	33.7	10.3
T2	50.0 ^{cd}	36.18 ^e	24.5	8.6
T3	50.0 ^{cd}	34.11 ^f	58.4	14.8
T4	83.3 ^b	82.14 ^a	34.4	7.9
T5	83.3 ^b	80.12 ^b	40.0	12.3
T6	33.3 ^d	27.34 ^g	61.4	13.9
T7	50.0 ^{cd}	55.32 ^d	31.4	9.6
T8	66.7 ^{bc}	25.43 ^h	50.3	12.1
T9	33.3 ^d	24.84 ^h	62.0	18.8
T10	33.3 ^b	36.15 ^b	38.5	10.2
T11	16.7 ^b	16.54 ^c	32.7	11.0
T12	16.7 ^b	3.25 ^g	50.6	16.2
T13	33.3 ^b	15.50 ^d	36.8	8.3
T14	33.3 ^b	13.42 ^{ef}	38.8	7.3
T15	0.00 ^c	0.00 ^h	38.0	8.7
T16	16.7 ^b	12.32 ^f	44.6	10.4
T17	16.7 ^b	14.23 ^{de}	38.9	9.7
T18	0.0 ^c	0.00 ^h	58.7	16.9
T19	100.0 ^a	78.43 ^c	37.5	9.7
T20	33.3 ^d	18.32 ⁱ	21.2	9.4
T21	0.00 ^e	0.00 ^j	41.9	6.9
LSD	19.19	1.03	5.371	2.645

Different letters in the same row mean significant difference. The significance level was set at $p < 0.05$.

Additionally, the combination of SiO₂, CuO, or Fe₂O₃ nanoparticles as a dipping and soil drench treatment proved to be the most effective strategy for controlling *Rhizoctonia* root rot caused by *R. solani*. Despite the low in vitro efficiency of SiO₂ nanoparticles, they showed considerable in vivo potential which may be attributed to the formation of physical barriers through Si accumulation in plant cells [44]. In addition to the direct effect of Fe₂O₃ nanoparticles on pathogen growth, they also induce higher activity of antioxidant enzymes due to iron involvement in enzyme activity and RNA synthesis [44]. CuO nanoparticles interact with microorganisms by permeating cell membranes, oxidizing membrane lipids, altering proteins, and denaturing nucleic acids, ultimately resulting in cell death [54].

3.6. Effect of Metal Oxide NPs on Soil Biological Activities

3.6.1. Effect on Microbial Community

Biotic and abiotic factors influence microbial populations both in terms of diversity and numbers in soil. These factors may include soil plant litter, root exudates, pathogens, management factors like mineral fertilizers, soil moisture, and soil organic matter, which in turn, affect crop production and the sustainability of soil health [55]. Therefore, we tested the population density of total mesophilic microflora and the principal enzymatic activities.

Data exhibited in Table 6 show that the highest bacterial count was observed with the 200 mg L⁻¹ SiO₂ dipping and soil drench method. However, at the same concentration, there was a notable decrease in the counts of silicate-solubilizing bacteria and *Azospirillum*, whereas the population of *Azotobacter* was stimulated. *Azotobacter* as an obligate aerobe is the predominant free-living diazotroph in soils [56]. Ref. [57] demonstrated that nanosilica significantly enhanced microbial populations, total biomass content, and silica content in maize. In particular, the population of phosphate-solubilizing bacteria (PSB) increased in soil treated with nanosilica, likely due to the increased availability of phosphorus, which is influenced by both phosphorus and silicon. Furthermore, the highest populations of nitrogen-fixing bacteria were observed in the nanosilica-treated soil, suggesting the

potential for increased nitrogen availability to plants through nitrogen fixation. However, the counts of sulfur-oxidizing bacteria (SSB) decreased.

Table 6. Microbial populations in the rhizosphere of lettuce plants infected with *Rhizoctonia solani* as affected by different concentrations of SiO₂, CuO, and γFe₂O₃ nanoparticles.

Treatments	T.B.C	T.F	T.Actin	PSB	SSB	<i>Azotobacter</i> sp.	<i>Azospirillum</i> sp.
	CFU × 10 ⁶	CFU × 10 ⁴	CFU × 10 ³	CFU × 10 ⁴	CFU × 10 ⁴	CFU × 10 ⁴	CFU × 10 ⁴
T1	9.47	10.33	5.67	10.33	0.84	1.05	0.37
T2	11.33	11.00	7.00	8.37	0.64	0.87	0.34
T3	12.87	11.67	7.33	10.27	0.84	1.13	0.33
T4	11.67	7.00	6.67	9.40	0.79	0.84	0.35
T5	14.33	4.00	6.00	9.14	0.90	0.86	0.31
T6	9.00	5.33	7.00	5.75	0.63	0.73	0.17
T7	20.33	14.33	10.33	8.70	0.85	0.76	0.30
T8	24.67	10.00	9.00	8.27	0.82	0.91	0.36
T9	17.33	8.00	13.33	11.20	0.87	0.71	0.21
T10	13.27	6.67	4.33	9.77	0.82	0.74	0.34
T11	12.17	10.00	5.67	7.77	0.71	0.90	0.06
T12	18.33	8.67	5.67	10.93	0.58	0.83	0.12
T13	19.64	6.67	3.33	8.07	0.87	0.87	0.42
T14	20.20	8.33	3.33	8.64	0.96	0.96	0.14
T15	11.40	8.67	2.67	4.73	0.47	0.70	0.08
T16	10.27	5.00	5.67	8.97	0.86	0.88	0.27
T17	9.87	5.00	3.67	7.33	0.87	0.69	0.24
T18	8.43	3.33	2.00	5.13	0.73	0.90	0.30
T19	13.87	14.67	3.00	5.13	0.58	0.81	0.14
T20	12.13	5.67	3.67	5.03	0.91	0.95	0.12
T21	10.33	10.67	6.00	8.83	0.99	0.71	0.44
LSD	2.324	2.612	1.729	2.463	0.236	0.142	0.111

T.B.C = total bacterial counts; T.F. = total fungi; T.Actin = total actinomycetes. PSB = phosphate-solubilizing bacteria; SSB = silicate-solubilizing bacteria, Cfu = colony-forming unit/g soil.

The different CuO NPs treatments caused significant changes in the microbial community structure. Treatments with 50 and 100 mg L⁻¹ CuO NPs resulted in a significant increase in bacterial count, actinomycetes, and free-living diazotrophs. However, the highest concentration of CuO NP (200 mg L⁻¹) led to a significant decrease in bacterial and actinomycetes counts. Surprisingly, there was no significant difference in phosphate-solubilizing bacteria (PSB) and sulfur-oxidizing bacteria (SSB) counts among CuO NP treatments up to 100 mg L⁻¹. However, a significant decrease was observed with the 200 mg L⁻¹ treatment. It is well known that elemental copper can be toxic to beneficial bacteria and fungi in the environment [58,59].

γFe₂O₃ NPs used for soil drenching generally increased total bacterial, actinomycetes, PSB, SSB, and free-living diazotroph counts. The maximum bacterial and free-living diazotroph counts were observed with 100 mgL⁻¹ Fe₂O₃ soil drench (T8) at 24.67 × 10⁶ and 0.91 × 10⁴ CFU/g dry soil, respectively. However, combined application treatments (dipping + soil drench) led to a significant decrease in total bacterial, actinomycetes, and fungal counts. Treatment with 200 mg L⁻¹ γFe₂O₃ NPs for soil drenching (T9) had a positive stimulation effect on beneficial soil microbes, with maximum bacterial numbers of 11.2, 0.87, 0.71, and 0.36 × 10⁴ CFU/g dry soil for PSB, SSB, and free-living diazotroph counts, respectively.

In a study by [60], the effect of magnetic iron oxide nanoparticles (Fe₃O₄ and γ-Fe₂O₃) on the soil bacterial community was investigated using molecular approaches. Results showed that the addition of these nanoparticles could stimulate bacterial growth and alter the community structure. Iron is an essential nutrient for microorganisms, as it is involved in cell growth and regulation through iron-sulfur (Fe-S) clusters. These clusters sense environmental signals, such as oxygen and iron levels, and mediate adaptive

responses [61]. The effects of magnetic iron oxide nanoparticles on bacterial populations can be related to both their properties and their impact on microbial metabolism [62,63]. Magnetic nanoparticles can easily penetrate soil due to their small size and stability, while their high surface-to-volume ratio makes them more prone to ion release compared to bulk materials. Additionally, nanoparticles have highly active surface sites, such as the Fe-OH site on iron oxide magnetic nanoparticles [29].

3.6.2. Effect on Soil Enzymatic Activities

Soil enzymatic activities reflect microbial performance and contribute to overall soil microbial activity [64,65]. Results illustrated in Figure 2 clearly indicated that, the combined treatment of dipping and soil drenching had the most significant effect, with a concentration of 200 mg L⁻¹ showing the highest impact, followed by 100 mg L⁻¹, while 50 mg L⁻¹ had the least significant effect. The highest dehydrogenase activity was observed with 50 mg L⁻¹ CuO NPs (dipping + soil drenching), followed by 100 mg L⁻¹ γ Fe₂O₃ NPs (dipping + soil drenching) and 200 mg L⁻¹ SiO₂ NPs (dipping + soil drenching) [66]. Alkaline phosphatase activity was significantly influenced by combined treatments of metal oxide NPs (dipping + soil drenching), with 200 mg L⁻¹ γ Fe₂O₃ NPs showing the highest activity. SiO₂ and CuO NPs decreased alkaline phosphatase activity compared to the control treatment. Phosphatases are a group of enzymes that are of great agronomic value because they catalyze the hydrolysis of organic phosphorus compounds and transform them into an inorganic form which is assimilated by plants and microorganisms [66]. γ Fe₂O₃ and CuO NPs stimulated urease activity, especially when applied through combined treatments. The highest urease activity was observed with 100 mg L⁻¹ γ Fe₂O₃ NPs (dipping + soil drenching) and 100 mg L⁻¹ CuO NPs (dipping + soil drenching). SiO₂ NPs had no significant effect on urease activity. All tested metal oxide NPs significantly stimulated soil nitrogenase activity, with SiO₂ NPs showing the highest activity at a concentration of 200 mg L⁻¹ (dipping + soil drenching). There was a direct correlation between SiO₂ NPs concentration and nitrogenase activity [66].

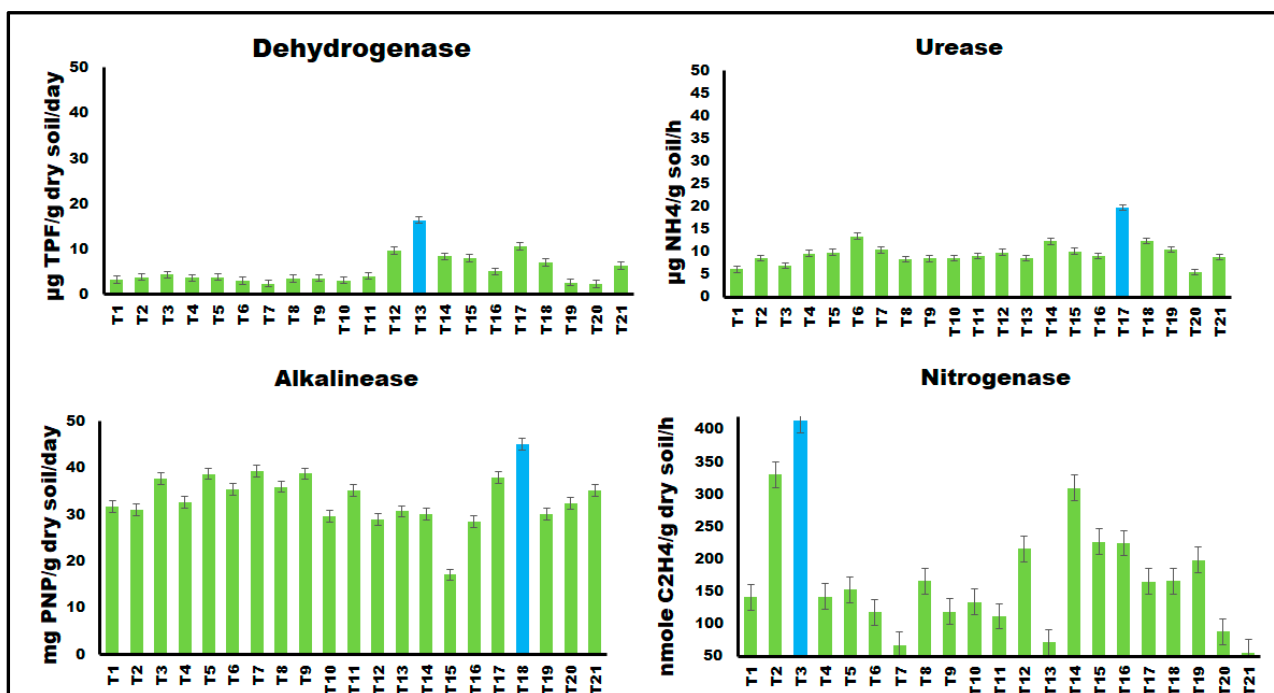


Figure 2. Soil enzymatic activity of dehydrogenase, urease, alkaline phosphatase and nitrogenase in the rhizosphere of lettuce plants infected with *Rhizoctonia solani* and treated with different concentrations of SiO₂, CuO, and γ Fe₂O₃ nanoparticles. Columns with blue indicate the highest activity.

These findings suggest that $\gamma\text{Fe}_2\text{O}_3$ NPs can enhance dehydrogenase, alkaline phosphatase, and urease activities through changes in the bacterial community. Iron is important for microorganisms as it acts as a cofactor for many enzymes [60,67]. CuO NPs have been shown to inhibit soil enzyme activities, including dehydrogenase, acid and alkaline phosphatase, and urease [68,69].

The positive impact of nanosilicon dioxide (SiO_2) and plant growth-promoting rhizobacteria (PGPR) on soil and plant health through increased microbial population and enzyme activity is consistent with previous research [70,71]. However, the effects of nanomaterials depend on various factors (NPs type, concentration, size, shape, exposure duration, and plant/animal species [71]).

3.7. Effect of Metal Oxide NPs on Endogenous Factors

The impact of metal oxide NPs (SiO_2 , CuO, and $\gamma\text{Fe}_2\text{O}_3$) on endogenous factors in plant growth and development was assessed by measuring various physiological parameters, including total chlorophyll, chlorophyll a, chlorophyll b, carotenoid content, cell membrane stability index (MDA), and rate of membrane leakage.

3.7.1. NPs Effect on Photosynthetic Pigments

Metal oxide NP treatments were assessed for their impact on photosynthetic pigments, which serve as indicators of plant stress [72]. As shown in Figure 3, without nanomaterials, *R. solani* bottom rot disease caused a significant reduction in total chlorophyll (35.66%) and carotenoid content (50.41%) (T19). $\gamma\text{Fe}_2\text{O}_3$ NPs at 50 mg L^{-1} (soil drench) significantly increased the total chlorophylls (82.2%) and carotenoids (67.22%) (T7). Significant increases were also observed with 200 mg L^{-1} CuO-NPs (dipping) in total chlorophylls (70.24%) and carotenoids (78.47%) (T6). SiO_2 -NPs had no adverse effects on photosynthetic pigments at lower concentrations (50 and 100 mg L^{-1}), but at 200 mg L^{-1} , they reduced chlorophyll content (Figure 4). Iron and copper are essential elements for photosynthetic efficiency and growth, while silica stimulates chlorophyll biosynthesis and activity [73–75]. Metal NPs enhance chlorophyll structure and metabolic activities [75]. Copper promotes plant growth but inhibits it at higher doses [59]. In a recent study by [76], foliar or soaking treatment of wheat plants with CuO-NPs at 50 ppm increased total chlorophylls (23% and 10.5%) and carotenoids (20.2% and 12.3%). This increase in photosynthesis rate may be due to the increased biological and chemical activities of metals at the nanoscale and the correlative impact of nutrients such as magnesium, iron, zinc, sulfur, etc., on plants. Silica stimulates chlorophyll biosynthesis and improves photosystem II activity [75].

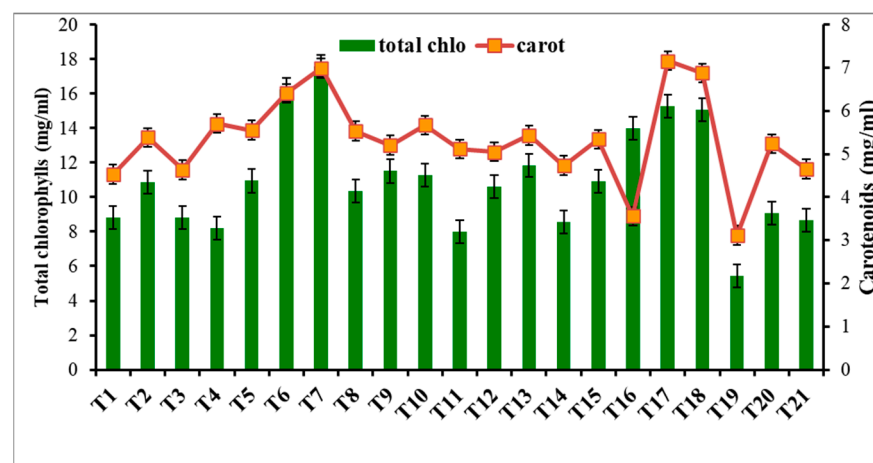


Figure 3. Effect of metal oxide NPs on total chlorophyll and carotenoid contents.

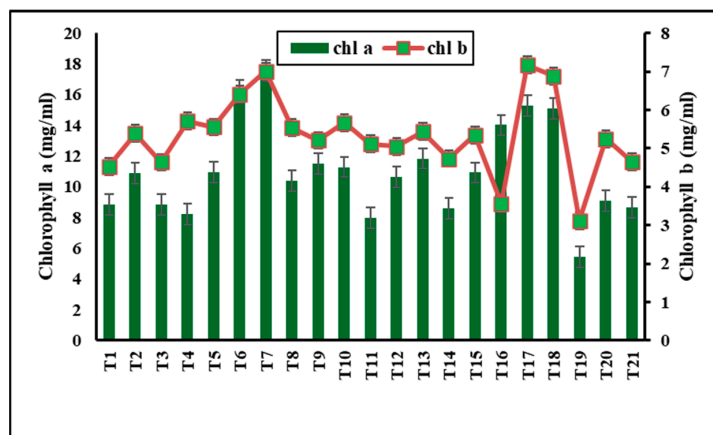


Figure 4. Effect of metal oxide NPs on chlorophyll a, chlorophyll b contents.

3.7.2. Effect of Metal oxide NPs on Malondialdehyde (MDA) and Electrolyte Leakage (EC)

Root rot infection often leads to increased lipid peroxidation, as indicated by elevated levels of malondialdehyde (MDA) and other aldehydes [72].

However, in the case of lettuce plants, the application of 50 mg L^{-1} $\gamma\text{Fe}_2\text{O}_3$ nanoparticles (NPs) as a soil drench treatment (T7) resulted in the most significant reduction in MDA levels (Figure 5). The combined treatment of dipping and soil drenching with $\gamma\text{Fe}_2\text{O}_3$ NPs showed a greater decrease in MDA levels compared to other treatments. Similarly, a soil drench treatment with 200 mg L^{-1} CuO NPs (T6) significantly decreased MDA levels. Conversely, SiO_2 -NPs treatments had a negative impact on MDA levels compared to the control (T1), indicating their potential to exacerbate lipid peroxidation under stress conditions.

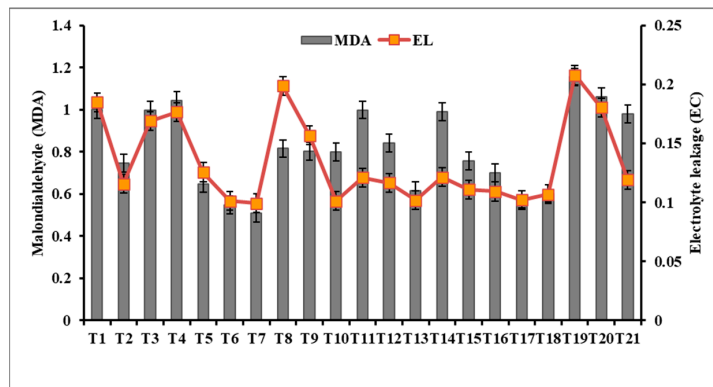


Figure 5. Effect of metal oxide NPs on malondialdehyde (MDA) and electrolyte leakage (EC).

To assess membrane permeability and electrolyte leakage caused by *Rhizoctonia solani* bottom rot infection and the impact of metal oxide NPs treatments, electrolyte leakage was measured after 60 days. The dipping and soil drench treatments with 50 mg L^{-1} $\gamma\text{Fe}_2\text{O}_3$ NPs (T10) exhibited the highest reduction in electrolyte leakage, which was consistent with the results of total chlorophylls, carotenoids, and MDA analysis. The most effective concentration of CuO NPs was found in T6, where a soil drench treatment of 200 mg L^{-1} CuO NPs was applied [70]. In contrast, SiO_2 -NPs treatments, especially the 200 mg L^{-1} SiO_2 -NPs soil drench treatment (T3), resulted in a significant increase in electrolyte leakage, indicating changes in membrane permeability [45]. Nanoparticles have shown potential in mitigating various stresses in plants, as demonstrated by the positive effects of iron oxide nanoparticles (IONPs) and silicon nanoparticles (SiNPs) in alleviating the effects of cadmium stress in *Phaseolus vulgaris* plants, including reducing MDA content and electrolyte leakage [70].

3.8. Anatomical Structure of Lettuce Root Infected with *R. solani* and Treated with Nano Metal Oxide

The control root (healthy plant) displayed a diameter of $680.957\ \mu\text{m}$ at $500\ \mu\text{m}$ depth (Figure 6a). The epidermis and cortical cells were intact, while the xylem vessels and phloem tissue were well developed. In contrast, the *R. solani*-infected control root (Figure 6b) exhibited hyphal growth along the epidermal walls, tissue disintegration, and disrupted xylem vessels. Crystal violet staining revealed substance accumulation on the infected control root walls. SiO_2 NPs treatment showed a slight decrease in root diameter ($464.466\ \mu\text{m}$) but improved phloem development when used as a dipping treatment. Combined dipping and soil drenching of SiO_2 NPs resulted in a larger root diameter ($657.726\ \mu\text{m}$) and well-defined tissue structure (Figure 6e). CuO NPs treatment increased the root diameter ($792.395\ \mu\text{m}$) but caused deformation and crushed the phloem tissue. The anatomical study demonstrated the toxic effect of a $200\ \text{mg L}^{-1}$ CuO NPs dipping and soil drenching treatment (T15). $\gamma\text{-Fe}_2\text{O}_3$ NPs treatment for soil drenching or combined dipping and soil drenching improved the root diameter ($752.00\ \mu\text{m}$ and $603.782\ \mu\text{m}$, respectively) and exhibited well-developed phloem tissue and visible primary xylem (Figure 6e,f).

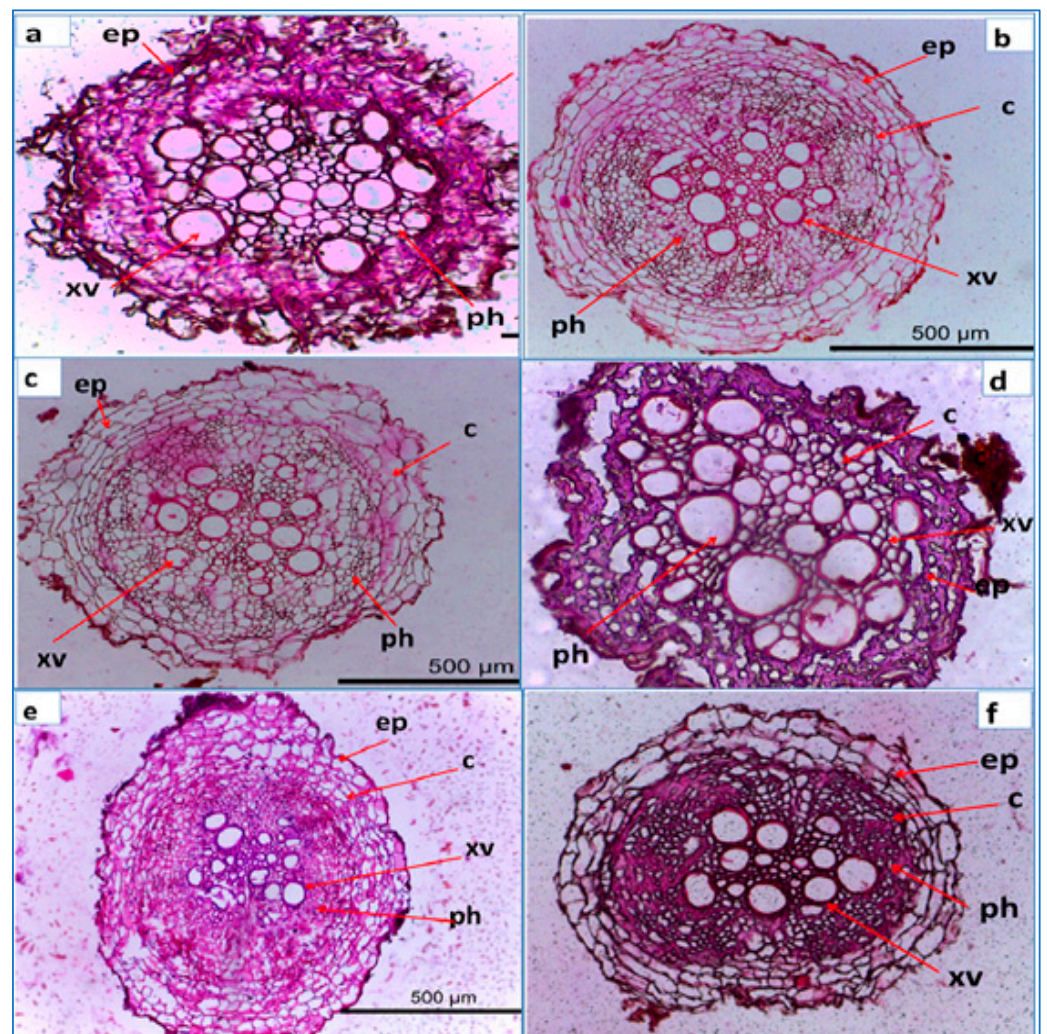


Figure 6. Light micrographs of cross-section of the root of lettuce inoculated with *R. solani* and treated with different nano metal oxides, (a) treated with SiO_2 for soil drenching; (b) SiO_2 for soil drenching + dipping; (c) CuO for soil drenching; (d) CuO for soil drenching + dipping; (e) $\gamma\text{Fe}_2\text{O}_3$ for soil drenching; (f) $\gamma\text{Fe}_2\text{O}_3$ for soil drenching + dipping. The abbreviations shown in the images refer to epidermis (ep), cortex (c), xylem vessel (xv), phloem tissue (ph). Transverse section of the root of lettuce under $20\times$ magnification. Bar = $500\ \mu\text{m}$.

Overall, SiO₂ NPs treatment enhanced phloem development, CuO NPs treatment increased root diameter but had adverse effects on tissue structure, and γ -Fe₂O₃ NPs treatment improved root diameter and mineral translocation. These findings highlight the potential of nano metal oxide treatments in promoting plant growth and resistance to *R. solani* infection.

4. Conclusions

This study underscores the urgent issue of fungal pathogens on crop yields, emphasizing the critical need for innovative and eco-friendly fungicide alternatives. The investigation into the in vitro effectiveness of SiO₂, CuO, and γ -Fe₂O₃ nanoparticles against *Rhizoctonia solani* showcases promising results. Particularly, the combined treatment of 200 mg L⁻¹ γ -Fe₂O₃ or CuO nanoparticles demonstrated exceptional in vitro antifungal activity. Furthermore, the in vivo impact of these nanoparticles, with two application methods, revealed additional insights into their potential benefits. γ -Fe₂O₃ nanoparticles, in particular, exhibited a range of positive effects, including enhanced plant photosynthetic pigments, reduced oxidative stress, and improved root anatomical features. These findings underscore the potential of γ -Fe₂O₃ nanoparticles as a sustainable alternative for managing crop diseases, opening doors to more effective and environmentally responsible agricultural practices.

Supplementary Materials: The following supporting information can be downloaded at: <https://www.mdpi.com/article/10.3390/microbiolres15010014/s1>, Figure S1. SEM images of Nano-SiO₂ (a), Nano- γ -Fe₂O₃ (b) and Nano-Copper (c).

Author Contributions: The collaborative efforts of the authors were integral to this research. N.A.H.F., T.A.E. and T.M.S. contributed significantly to the conceptualization and methodology. Alongside A.A.T., S.F.E. and N.A.T., they played crucial roles in developing and validating the methodology. T.A.E. and T.E. handled software implementation and validation. N.A.H.F., T.A.E. and T.E. conducted data analysis, while investigation efforts were shared by N.A.H.F., T.A.E. and N.A.T., N.A.H.F. and T.A.E. managed project resources, and data curation involved N.A.H.F., T.A.E. and T.E. The manuscript's initial draft was collaboratively written by N.A.H.F., T.M.S., T.A.E. and T.E., with T.E. taking the lead in review and editing. Visualization tasks were shared by N.A.H.F., T.A.E. and T.E., and project supervision was led by N.A.H.F. and T.E. All authors have read and agreed to the published version of the manuscript.

Funding: This research received no external funding.

Institutional Review Board Statement: This research study does not involve the use of human subjects. As such, it falls outside the purview of the Institutional Review Board (IRB) requirements.

Informed Consent Statement: This research study does not involve the use of human or animal samples. As such, the requirement for informed consent is not applicable.

Data Availability Statement: The original contributions presented in the study are included in the article/supplementary material, further inquiries can be directed to the corresponding author/s.

Conflicts of Interest: The authors declare no conflict of interest.

References

1. Raza, A.; Razzaq, A.; Mehmood, S.S.; Zou, X.; Zhang, X.; Lv, Y.; Xu, J. Impact of climate change on crops adaptation and strategies to tackle its outcome: A review. *Plants* **2019**, *8*, 34. [[CrossRef](#)] [[PubMed](#)]
2. Passarelli, M.; Bongiorno, G.; Cucino, V.; Cariola, A. Adopting new technologies during the crisis: An empirical analysis of agricultural sector. *Technol. Forecast. Soc. Chang.* **2023**, *186*, 122106. [[CrossRef](#)]
3. Shang, Y.; Hasan, M.K.; Ahammed, G.J.; Li, M.; Yin, H.; Zhou, J. Applications of Nanotechnology in Plant Growth and Crop Protection: A Review. *Molecules* **2019**, *24*, 2558. [[CrossRef](#)] [[PubMed](#)]
4. Khan, M.; Khan, A.U.; Hasan, M.A.; Yadav, K.K.; Pinto, M.M.C.; Malik, N.; Yadav, V.K.; Khan, A.H.; Islam, S.; Sharma, G.K. Agro-nanotechnology as an emerging field: A novel sustainable approach for improving plant growth by reducing biotic stress. *Appl. Sci.* **2021**, *11*, 2282. [[CrossRef](#)]
5. Grillo, R.; Abhilash, P.C.; Fraceto, L.F. Nanotechnology applied to bio-encapsulation of pesticides. *J. Nanosci. Nanotechnol.* **2016**, *16*, 1231–1234. [[CrossRef](#)] [[PubMed](#)]

6. Kah, M.; Tufenkji, N.; White, J.C. Nano-enabled strategies to enhance crop nutrition and protection. *Nat. Nanotechnol.* **2019**, *14*, 532–540. [[CrossRef](#)] [[PubMed](#)]
7. Massalimov, I.; Ram, P.; Amr, I.M.I.; Ahmed, I.S.A. *Modern Prospects of Nanotechnology in Plant Pathology*; Springer: Berlin/Heidelberg, Germany, 2017; pp. 1–372. [[CrossRef](#)]
8. Wolf, P.F.J.; Lenz, R.; Baron, K.; Verreet, J.A. Quaternary integrated pest management concept for powdery mildew in sugar beet. I. Analysis of epidemic determinants to predict disease onset. *J. Plant Dis. Prot.* **2006**, *113*, 61–67. [[CrossRef](#)]
9. Elshahawy, I.E.; El-Mohamedy, R.S. Biological control of Pythium damping-off and root-rot diseases of tomato using Trichoderma isolates employed alone or in combination. *J. Plant Pathol.* **2019**, *101*, 597–608. [[CrossRef](#)]
10. Wallon, T.; Sauvageau, A.; Van der Heyden, H. Detection and quantification of rhizoctonia solani and rhizoctonia solani ag1-ib causing the bottom rot of lettuce in tissues and soils by multiplex qpcr. *Plants* **2021**, *10*, 57. [[CrossRef](#)]
11. Martins, S.A.; Schurt, D.A.; Seabra, S.S.; Martins, S.J.; Ramalho, M.A.P.; Moreira, F.M.d.S.; da Silva, J.C.P.; da Silva, J.A.G.; de Medeiros, F.H.V. Common bean (*Phaseolus vulgaris* L.) growth promotion and biocontrol by rhizobacteria under Rhizoctonia solani suppressive and conducive soils. *Appl. Soil Ecol.* **2018**, *127*, 129–135. [[CrossRef](#)]
12. Mondal, P.; Kumar, R.; Gogoi, R. Bioorganic Chemistry fungicidal evaluation against *Sclerotium rolfsii*, *Rhizoctonia bataticola* and *Rhizoctonia solani*. *Bioorg. Chem.* **2017**, *70*, 153–162. [[CrossRef](#)] [[PubMed](#)]
13. Raghupati, K.R.; Koodali, R.T.; Manna, A.C. Size-dependent bacterial growth inhibition and mechanism of antibacterial activity of zinc oxide nanoparticles. *Langmuir* **2011**, *27*, 4020–4028. [[CrossRef](#)]
14. Jones, N.; Ray, B.; Ranjit, K.T.; Manna, A.C. Antibacterial activity of ZnO nanoparticles suspensions on a broad spectrum of microorganisms. *FEMS Microbiol. Lett.* **2008**, *279*, 71–76. [[CrossRef](#)]
15. Azam, A.; Ahmed, A.S.; Oves, M.; Khan, M.S.; Habib, S.S.; Memic, A. Antimicrobial activity of metal oxide nanoparticles against Gram-positive and Gram-negative bacteria: A comparative study. *Int. J. Nanomed.* **2012**, *7*, 6003–6009. [[CrossRef](#)]
16. Subhapiya, S.; Gomathipriya, P. Green synthesis of titanium dioxide (TiO₂) nanoparticles by Trigonella foenum-graecum extract and its antimicrobial properties. *Microb. Pathog.* **2018**, *116*, 215–220. [[CrossRef](#)] [[PubMed](#)]
17. Tortella, G.; Rubilar, O.; Pieretti, J.C.; Fincheira, P.; de Melo Santana, B.; Fernández-Baldo, M.A.; Benavides-Mendoza, A.; Seabra, A.B. Nanoparticles as a Promising Strategy to Mitigate Biotic Stress in Agriculture. *Antibiotics* **2023**, *12*, 338. [[CrossRef](#)]
18. Day, J.M.; Döbereiner, J. Physiological aspects of N₂-fixation by a Spirillum from Digitaria roots. *Soil Biol. Biochem.* **1976**, *8*, 45–50. [[CrossRef](#)]
19. Xiong, L.; Tong, Z.H.; Chen, J.J.; Li, L.L.; Yu, H.Q. Morphology-dependent antimicrobial activity of Cu/Cu₂O nanoparticles. *Ecotoxicology* **2015**, *24*, 2067–2072. [[CrossRef](#)]
20. Khatami, M.; Varma, R.; Heydari, M.; Peydayesh, M.; Sedighi, A.; Askari, H.A.; Rohani, M.; Baniasadi, M.; Arkia, S.; Seyedi, F.; et al. Copper oxide nanoparticles greener synthesis using tea and its antifungal efficiency on Fusarium solani. *Geomicrobiol. J.* **2019**, *36*, 777–781. [[CrossRef](#)]
21. Kamel, S.M.; Elgobashy, S.F.; Omara, R.I.; Derbalah, A.S.; Abdelfatah, M.; El-Shaer, A.; Al-Askar, A.A.; Abdelkhalek, A.; Abd-El salam, K.A.; Essa, T.; et al. Antifungal Activity of Copper Oxide Nanoparticles against Root Rot Disease in Cucumber. *J. Fungi* **2022**, *8*, 911. [[CrossRef](#)]
22. Elmer, W.H.; De La Torre-Roche, R.; Pagano, L.; Majumdar, S.; Zuverza-Mena, N.; Dimpka, C.; Gardea-Torresdey, J.; White, W. Effect of metalloids and metallic oxide nanoparticles on Fusarium wilt of watermelon. *Plant. Dis.* **2018**, *102*, 1394–1401. [[CrossRef](#)]
23. El-Batal, A.I.; El-Sayyad, G.S.; Al-Shammari, B.M.; Abdelaziz, A.M.; Nofel, M.M.; Gobara, M.; Elkhatib, W.F.; Eid, N.A.; Salem, M.S.; Attia, M.S. Protective role of iron oxide nanocomposites on disease index, and biochemical resistance indicators against Fusarium oxysporum induced-cucumber wilt disease: In vitro, and in vivo studies. *Microb. Pathog.* **2023**, *180*, 106131. [[CrossRef](#)] [[PubMed](#)]
24. Filho, J.A.W.; Duarte, H.S.S.; Rodrigues, F.A. Effect of foliar application of potassium silicate and fungicide on the severity of leaf rust and yellow leaf spot in wheat. *Rev. Ceres* **2013**, *60*, 726–730.
25. Rodrigues, F.A.; Dallagnol, L.J.; Duarte, H.S.S.; Datnoff, L.E. Silicon control of foliar diseases in monocots and dicots. In *Silicon and Plant Diseases*; Springer International Publishing: Cham, Switzerland, 2015.
26. Abdelrhim, A.S.; Mazrou, Y.S.A.; Nehela, Y.; Atallah, O.O.; El-Ashmony, R.M.; Dawood, M.F.A. Silicon Dioxide Nanoparticles Induce Innate Immune Responses and Activate Antioxidant Machinery in Wheat against Rhizoctonia solani. *Plants* **2021**, *10*, 2758. [[CrossRef](#)] [[PubMed](#)]
27. Ainsworth, G.C.; James, P.W. *Ainsworth and Bisby's Dictionary of Fungi*, 6th ed.; Commonwealth Mycological Institute: Kew, UK, 1971.
28. Alexopoulos, C.J.; Mims, C.W.; Blackwell, M. *Introductory Mycology*, 4th ed.; John Wiley and Sons: New York, NY, USA, 1996.
29. Liu, S.; Wei, L.; Hao, L.; Fang, N.; Chang, M.W.; Xu, R.; Yang, Y.; Chen, Y. Sharper and faster “Nano darts” kill more bacteria: A study of antibacterial activity of individually dispersed pristine single-walled carbon nanotube. *ACS Nano* **2009**, *3*, 3891–3902. [[CrossRef](#)]
30. Abd-El-Khair, H.; El-Nagdi, W.M.A. Field application of bio-control agents for controlling fungal root rot and root-knot nematode in potato. *Arch. Phytopathol. Plant Prot.* **2014**, *47*, 1218–1230. [[CrossRef](#)]
31. Fratemale, D.; Giamperi, L.; Ricci, D. Chemical Composition and antifungal activity of essential oil obtained from in vitro plants of *Thymus mastichina* L. *J. Essent. Oil Res.* **2003**, *15*, 278–281. [[CrossRef](#)]

32. Wang, Q.; Xiong, D.; Zhao, P.; Yu, X.; Tu, B.; Wang, G. Effect of applying an arsenic-resistant and plant growth-promoting rhizobacterium to enhance soil arsenic phytoremediation by *Populus deltoides* LH05-17. *J. Appl. Microbiol.* **2011**, *111*, 1065–1074. [CrossRef]
33. Black, C.A. *Methods of Soil Analysis. Part 2. Chemical and Microbiological Properties*, 2nd ed.; American Society of Agronomy: Madison, WI, USA, 1982.
34. Atlas, R.M. *Handbook of Microbiological Media for the Examination of Food*; CRC Press: Boca Raton, FL, USA, 1995.
35. Difco. *Difco & BBL Manual: Manual of Microbiological Culture Media*, 2nd ed.; Citeseer: College Park, MD, USA, 2009. [CrossRef]
36. Döbereiner, J.; Day, J.M.; Dart, P.J. Nitrogenase activity in the rhizosphere of sugar cane and some other tropical grasses. *Plant Soil* **1972**, *37*, 191–196. [CrossRef]
37. Abd-el-Malek, Y.; Ishac, Y.Z. Evaluation of Methods Used in Counting Azotobacters. *J. Appl. Bacteriol.* **1968**, *31*, 267–275. [CrossRef]
38. Pikovskaya, R.I. Mobilization of phosphorus in soil connection with the vital activity of some microbial species. *Microbiologiya* **1984**, *17*, 362–370.
39. Zahra, M.K. Studies of Silicate Bacteria. Master's Thesis, Faculty of Agriculture Cairo University, Giza, Egypt, 1969; p. 111.
40. Casida, L.E., Jr. Microbial Metabolic Activity in Soil as Measured by Dehydrogenase Determination. *Appl. Environ. Microbiol.* **1977**, *34*, 630–636. [CrossRef]
41. Tabatabai, M.A.; Bremner, J.M. Assay of urease activity in soils. *Soil Biol. Biochem.* **1972**, *4*, 479–487. [CrossRef]
42. Senwo, Z.N.; Ranatunga, T.D.; Tazisong, I.A.; Taylor, R.W.; He, Z. Phosphatase activity of Ultisols and relationship to soil fertility indices. *J. Food Agric. Environ.* **2007**, *5*, 262–266.
43. Young, A.J. The photoprotective role of carotenoids in higher plants. *Physiol. Plant.* **1991**, *83*, 702–708. [CrossRef]
44. Zedan, A.; Omar, S. Nano selenium: Reduction of severe hazards of atrazine and promotion of changes in growth and gene-expression patterns on *Vicia faba* seedlings. *Afr. J. Biotechnol.* **2019**, *18*, 502–510.
45. Blokhina, O.; Virolainen, E.; Fagerstedt, K.V. Antioxidants, oxidative damage and oxygen deprivation stress: A review. *Ann. Bot.* **2003**, *91*, 179–194. [CrossRef]
46. Saeed, M.; Dodd, P.B.; Sohail, L. Anatomical studies of stems, roots and leaves of.pdf. *J. Hortic. For.* **2010**, *2*, 87–94.
47. Hoshmand, A. *Design of Experiments for Agriculture and the Natural Sciences*, 2nd ed.; Chapman and Hall: New York, NY, USA, 2006.
48. Premaratne, W.A.P.J.; Priyadarshana, W.M.G.I.; Gunawardena, S.H.P.; De Alwis, A.A.P. Synthesis of nanosilica from paddy husk ash and their surface functionalization. *J. Sci. Univ. Kelaniya Sri Lanka* **2013**, *8*, 33–48. [CrossRef]
49. Jeon, C.S.; Baek, K.; Park, J.K.; Oh, Y.K.; Lee, S.D. Adsorption characteristics of As (V) on iron-coated zeolite. *J. Hazard. Mater.* **2009**, *163*, 804–808. [CrossRef]
50. Chen, J.P.; Lim, L.L. Key Factors in Chemical Reduction by Hydrazine for Recovery of Precious Metals. *Chemosphere* **2002**, *49*, 363–370. [CrossRef] [PubMed]
51. Khan, A.; Rashid, A.; Younas, R.; Chong, R. A chemical reduction approach to the synthesis of copper nanoparticles. *Int. Nano Lett.* **2016**, *6*, 21–26. [CrossRef]
52. Raghunath, A.; Perumal, E. Metal oxide nanoparticles as antimicrobial agents: A promise for the future. *Int. J. Antimicrob. Agents* **2017**, *49*, 137–152. [CrossRef] [PubMed]
53. Xie, Y.; He, Y.; Irwin, P.L.; Jin, T.; Shi, X. Antibacterial activity and mechanism of action of zinc oxide nanoparticles against *Campylobacter jejuni*. *Appl. Environ. Microbiol.* **2011**, *77*, 2325–2331. [CrossRef] [PubMed]
54. Oussou-Azo, A.F.; Nakama, T.; Nakamura, M.; Futagami, T.; Vestergaard, M.C.M. Antifungal potential of nanostructured crystalline copper and its oxide forms. *Nanomaterials* **2020**, *10*, 1003. [CrossRef] [PubMed]
55. Nashwa, A.H.F.; Mervat, A.H. Reduction of Urea Transformation in Soil Using Aqueous Extracted Leaves of Neem (*Azadirachta indica*) and Olive (*Olea europaea* L). *Indian J. Environ. Prot. IJEP* **2020**, *40*, 12–22. Available online: <https://www.e-ijep.co.in/january-2020/> (accessed on 15 January 2023).
56. Nashwa, A.H.F.; Massoud, O.N.; Ebtsam, M.M.; Khalil, H.M. Biological Evaluation of Soil Cultivated with Egyptian Clover (*Trifolium alexandrinum* L.) through Long Term Trial at Bahtim Region, Egypt. *Sciences* **2015**, *5*, 515–525. Available online: <https://www.curreweb.com/mejas/mejas/2015/515-525.pdf> (accessed on 12 May 2023).
57. Rangaraj, S.; Gopalu, K.; Rathinam, Y.; Periasamy, P.; Venkatachalam, R.; Narayanasamy, K. Effect of silica nanoparticles on microbial biomass and silica availability in maize rhizosphere. *Biotechnol. Appl. Biochem.* **2014**, *61*, 668–675. [CrossRef]
58. Díaz-Raviña, M.; de Anta, R.C.; Bååth, E. Tolerance (PICT) of the Bacterial Communities to Copper in Vineyards Soils from Spain. *J. Environ. Qual.* **2007**, *36*, 1760–1764. [CrossRef]
59. Bakshi, M.; Kumar, A. Copper-based nanoparticles in the soil-plant environment: Assessing their applications, interactions, fate and toxicity. *Chemosphere* **2021**, *281*, 130940. [CrossRef]
60. He, S.; Feng, Y.; Ren, H.; Zhang, Y.; Gu, N.; Lin, X. The impact of iron oxide magnetic nanoparticles on the soil bacterial community. *J. Soils Sediments* **2011**, *11*, 1408–1417. [CrossRef]
61. Xu, J.; Chen, Y.; Luo, J.; Xu, J.; Zhou, G.; Yu, Y.; Xue, L.; Yang, L.; He, S. Fe₃O₄ nanoparticles affect paddy soil microbial-driven carbon and nitrogen processes: Roles of surface coating and soil types. *Environ. Sci. Nano* **2022**, *9*, 2440–2452. [CrossRef]
62. Ju-Nam, Y.; Lead, J.R. Manufactured nanoparticles: An overview of their chemistry, interactions and potential environmental implications. *Sci. Total Environ.* **2008**, *400*, 396–414. [CrossRef] [PubMed]
63. Nowack, B. The behavior and effects of nanoparticles in the environment. *Environ. Pollut.* **2009**, *157*, 1063–1064. [CrossRef]

64. Khalifa, M.; Fetyan, N.A.H.; Magid, M.S.A.; El-Sherry, N.I. Effectiveness of potassium silicate in suppression white rot disease and enhancement physiological resistance of onion plants, and its role on the soil microbial community. *Middle East J. Agric. Res.* **2017**, *6*, 376–394.
65. Stone, M.M.; DeForest, J.L.; Plante, A.F. Changes in extracellular enzyme activity and microbial community structure with soil depth at the Luquillo Critical Zone Observatory. *Soil Biol. Biochem.* **2014**, *75*, 237–247. [[CrossRef](#)]
66. Bandick, A.K.; Dick, R.P. Field management effects on soil enzyme activities. *Soil Biol. Biochem.* **1999**, *31*, 1471–1479. [[CrossRef](#)]
67. Outten, F.W.; Theil, E.C. Iron-based redox switches in biology. *Antioxid. Redox Signal.* **2009**, *11*, 1029–1046. [[CrossRef](#)]
68. Asadishad, B.; Chahal, S.; Akbari, A.; Cianciarelli, V.; Azodi, M.; Ghoshal, S.; Tufenkji, N. Amendment of Agricultural Soil with Metal Nanoparticles: Effects on Soil Enzyme Activity and Microbial Community Composition. *Environ. Sci. Technol.* **2018**, *52*, 1908–1918. [[CrossRef](#)]
69. Joško, I.; Oleszczuk, P.; Futa, B. The effect of inorganic nanoparticles (ZnO, Cr₂O₃, CuO and Ni) and their bulk counterparts on enzyme activities in different soils. *Geoderma* **2014**, *232–234*, 528–537. [[CrossRef](#)]
70. Kukreti, B.; Sharma, A.; Chaudhary, P.; Agri, U.; Maithani, D. Influence of nanosilicon dioxide along with bioinoculants on Zea mays and its rhizospheric soil. *3 Biotech* **2020**, *10*, 345. [[CrossRef](#)] [[PubMed](#)]
71. Naushad, M. Surfactant assisted nano-composite cation exchanger: Development, characterization and applications for the removal of toxic Pb²⁺ from aqueous medium. *Chem. Eng. J.* **2014**, *235*, 100–108. [[CrossRef](#)]
72. Zhao, W.; Liu, L.; Shen, Q.; Yang, J.; Han, X.; Tian, F.; Wu, J. Effects of water stress on photosynthesis, yield, and water use efficiency in winter wheat. *Water* **2020**, *12*, 2127. [[CrossRef](#)]
73. Briat, J.F.; Duc, C.; Ravet, K.; Gaymard, F. Ferritins and iron storage in plants. *Biochim. Biophys. Acta Gen. Subj.* **2010**, *1800*, 806–814. [[CrossRef](#)]
74. Aguirre, G.; Pilon, M. Copper delivery to chloroplast proteins and its regulation. *Front. Plant Sci.* **2016**, *6*, 1250. [[CrossRef](#)]
75. Jurkow, R.; Sekara, A.; Pokluda, R.; Smoleń, S.; Kalisz, A. Biochemical response of oakleaf lettuce seedlings to different concentrations of some metal(oid) oxide nanoparticles. *Agronomy* **2020**, *10*, 997. [[CrossRef](#)]
76. Badawy, A.A.; Abdelfattah, N.A.H.; Salem, S.S.; Awad, M.F.; Fouda, A. Efficacy assessment of biosynthesized copper oxide nanoparticles (CuO-nps) on stored grain insects and their impacts on morphological and physiological traits of wheat (*Triticum aestivum* L.) plant. *Biology* **2021**, *10*, 233. [[CrossRef](#)]

Disclaimer/Publisher’s Note: The statements, opinions and data contained in all publications are solely those of the individual author(s) and contributor(s) and not of MDPI and/or the editor(s). MDPI and/or the editor(s) disclaim responsibility for any injury to people or property resulting from any ideas, methods, instructions or products referred to in the content.